

# Measurements of submillimeter polarization induced by oblique reflection from aluminum alloy

Tom Renbarger, Jessie L. Dotson, and Giles Novak

We have measured the linear polarization induced in a beam of submillimeter radiation when it is obliquely reflected by a flat mirror made of aluminum alloy. For angles of incidence in the range  $15^\circ$ – $45^\circ$ , we measured induced polarizations in the range 0.05%–0.25%. Our measurements are within a factor of 2 of theoretical predictions. We conclude that astronomical telescopes that incorporate oblique reflections from good conductors will not introduce spurious polarizations large enough to cause significant problems for submillimeter polarimetric observations. © 1998 Optical Society of America

OCIS codes: 120.5410, 120.5700, 350.1260.

## 1. Introduction

Interstellar dust grains absorb optical starlight and reemit it primarily at far-infrared and submillimeter wavelengths. The grains rotate about their short axes, which tend to align with the direction of the interstellar magnetic field. This overall magnetic alignment produces a slight linear polarization in the thermal emission of the dust. The magnitude of this effect ranges from several tenths of a percent to  $\sim 10\%$ , with a median value of  $\sim 2\%$ .<sup>1</sup> By measuring the direction of polarization, one can infer the direction of the magnetic field projected onto the plane of the sky. This information helps in determining the role that magnetic fields play in interstellar processes. For example, magnetic fields are believed to influence star formation through angular momentum transfer and cloud support.<sup>2</sup> They may also play an important role in the dynamics of the circumnuclear ring at the center of this galaxy.<sup>3</sup>

To map magnetic fields successfully by far-infrared–submillimeter polarimetry, one needs to make polarization measurements with systematic errors of no more than a few tenths of a percent. Previous measurements characterized the instrumental polarization of far-infrared–submillimeter polarim-

eters sufficiently to reduce their systematic errors to an acceptable level.<sup>4,5</sup> To estimate the systematic errors that could be introduced by the use of off-axis telescopes, one must consider the polarization induced by oblique reflections from good conductors. We restrict ourselves to the case of submillimeter ( $\lambda \sim 250$ – $1000 \mu\text{m}$ ) wavelengths for the remainder of this paper. If the polarization by reflection at these wavelengths were to agree with the value predicted from the ordinary skin effect from classical electromagnetic theory,<sup>6</sup> then the magnitude of polarization induced by an off-axis telescope would be at the acceptable level of a few tenths of a percent.

A previous study shows that the polarization induced by oblique reflection from aluminum alloy at a wavelength of  $\sim 1 \text{ cm}$  agrees with the prediction of the ordinary skin effect.<sup>7</sup> Measurements at  $165 \mu\text{m}$  for aluminum and aluminum alloy have shown that the absorption from a  $45^\circ$  angle-of-incidence reflection is in the range of 0.7–1.0%.<sup>8</sup> This measured absorption is within 50% of the theoretically expected ordinary skin effect value.<sup>6,8</sup> As we show in Section 2, the absorptivity is related to the polarization. Although these results are thus encouraging for astronomical observations, direct measurements of polarization by reflection at submillimeter wavelengths would seem to be required for a more definitive characterization of the effects of oblique reflections. We present here the results of a set of measurements designed to investigate this issue.

In Section 2 we discuss predictions made by use of the ordinary skin effect theory. Section 3 details our experimental setup, procedure, and results. In Section 4 we discuss possible explanations for the discrepancy between the theoretical and the measured

---

The authors are with the Department of Physics and Astronomy, Northwestern University, 2131 Sheridan Road, Evanston, Illinois 60208-2900. (T. Renbarger's e-mail address is t-renbarger@nwu.edu.)

Received 18 February 1998; revised manuscript received 1 June 1998.

0003-6935/98/286643-05\$15.00/0

© 1998 Optical Society of America

polarizations, including absorptive loss owing to the anomalous skin effect<sup>9-14</sup> and absorptive<sup>15</sup> and scattering<sup>16</sup> losses owing to surface roughness. Finally, in Section 5 we consider the implications of our experiment for submillimeter-wavelength polarimetry of astronomical sources.

## 2. Theoretical Predictions

The general problem of predicting the polarization induced by oblique reflection from a good conductor reduces to finding the reflectivities (or absorptivities) of the two polarization components of the radiation as a function of the angle of incidence. Assuming reflection by a plane conductor, one can readily calculate the induced polarization by using the Fresnel formulas for the reflectivity of an imperfect conductor.<sup>6</sup>

For the preceding calculation to be valid, the current density must be proportional to the electric field in the conductor, with conductivity as the proportionality constant, as in the microscopic version of Ohm's law. If this condition is met, the calculation falls into the regime of the ordinary skin effect. When this relationship between current and field in the metal breaks down, conductivity cannot be treated as a local phenomenon, and a new method to calculate reflectivities is required. The theory of the anomalous skin effect<sup>9-14</sup> was developed for this purpose.

In this section we predict the polarization by reflection for the conditions that pertain to the measurement that we made. These conditions include a passband centered at 320  $\mu\text{m}$ , which corresponds to an angular frequency  $\omega = 5.89 \times 10^{12}$  Hz, with a relative bandwidth of 0.375, angles of incidence from 15° to 45°, and reflecting material Al 6061, with a dc conductivity  $\sigma = 2.31 \times 10^{17}$  Hz.<sup>17</sup> First, however, we show that we are in the regime of the ordinary skin effect rather than of the anomalous skin effect.

We consider the relative sizes of the following two length scales: the skin depth  $\delta$  and the mean free path of the conduction electrons,  $l$ . In the standard derivation of the ordinary skin effect one assumes that  $\delta \gg l$ , implying that electrons undergo many collisions in one skin depth, and one can treat conductivity as a local phenomenon. Should  $l > \delta$ , conductivity can no longer be treated in the familiar microscopic manner, and corrections that are due to the anomalous skin effect must be applied.

For Al 6061, at room temperature and  $\lambda = 320 \mu\text{m}$ ,  $\delta \sim 100$  nm and  $l \sim 11$  nm. We determined  $\delta$  by means of the ordinary skin effect calculation.<sup>6</sup> We calculated  $l$  from the free-electron model for conductivity based on the dc value of  $\sigma$  given above.<sup>18</sup> Inasmuch as  $\delta \sim 9l$ , the ordinary skin effect should give a reasonable approximation.

Before proceeding with the calculation of the ordinary skin effect one must consider whether any correction to conductivity arises as a result of the ac nature of the incident radiation, which one can determine by comparing  $l$  with a third length scale,  $v_F/\omega$ . The current that drives the reflected wave comprises free electrons moving at the Fermi velocity

$v_F$ . This third length scale can then be thought of as the distance that an electron travels in time  $\omega^{-1}$ , i.e., before the electric field changes direction. If  $v_F/\omega \gg l$ , then electrons undergo enough collisions before the field direction switches to permit any ac modifications to the bulk conductivity to be ignored. As  $l$  approaches  $v_F/\omega$  in magnitude, ac corrections begin to apply. For Al 6061,  $v_F \sim 2 \times 10^8$  cm/s,<sup>17,18</sup> yielding  $v_F/\omega \sim 350$  nm. Recalling that  $l \sim 11$  nm, we see that we can use the dc conductivity.

In the limit of a good conductor ( $\sigma \gg \omega$ ) and non-grazing incidence, the reflectivities are given (in cgs units) by

$$R_{\parallel} \approx 1 - 2\mu \cos \theta \left[ \left( \frac{\omega}{2\pi\mu\sigma} \right) \right]^{1/2}, \quad (1a)$$

$$R_{\perp} \approx 1 - \left( \frac{2\mu}{\cos \theta} \right) \left[ \left( \frac{\omega}{2\pi\mu\sigma} \right) \right]^{1/2}, \quad (1b)$$

where  $\theta$  is the angle of incidence,  $\omega$  is the angular frequency of the radiation,  $\mu$  is the magnetic permeability, and  $\sigma$  is the dc electrical conductivity.<sup>6</sup>  $R_{\parallel}$  is the reflectivity of the polarization component with the  $E$  vector lying in the plane of incidence, and  $R_{\perp}$  is the reflectivity of the polarization component with the  $E$  vector lying in the plane of the conductor. The polarization is given by

$$P = (R_{\perp} - R_{\parallel}) / (R_{\perp} + R_{\parallel}), \quad (2)$$

which simply becomes

$$P \approx \left[ \left( \frac{\omega\mu}{2\pi\sigma} \right) \right]^{1/2} \sin \theta \tan \theta \quad (3)$$

(as  $R_{\perp} + R_{\parallel} \approx 2$  and  $\sec \theta - \cos \theta = \sin \theta \tan \theta$ ). The direction of the induced polarization will be such that the  $E$  vector is parallel to the plane of the conductor. Note that the coefficient of approximation (3) is equal to half of the normal-incidence absorptivity as determined by the ordinary skin effect theory.

We note here that we made all our measurements with angles of incidence between 15° and 45°, where the expressions for the reflectivities are accurate. Were we to measure at grazing angles of incidence ( $\theta \geq 80^\circ$ ), we would require the exact expressions from which approximations (1a) and (1b) are derived.<sup>6</sup>

Using the values of frequency and conductivity given above, and assuming that  $\mu \sim 1$ , we predict a value of induced polarization  $P = (0.20\% \pm 0.02\%) \sin \theta \tan \theta$ . The uncertainty arises from uncertainty in the value of the conductivity for Al 6061 and from effects that are due to finite bandwidth.

## 3. Experimental Apparatus, Procedure, and Results

We measured the polarization induced by reflection from a plate of Al 6061 with a diameter of 6" (15.24 cm) and thickness of 1/4" (0.64 cm). The surface of the aluminum plate was cut on a lathe to a good machine finish with a groove spacing of a few micrometers. Figure 1 is a schematic illustration of

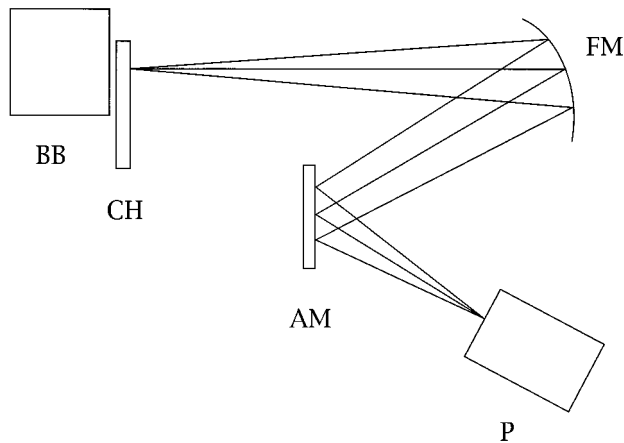


Fig. 1. Schematic diagram of the experiment. The view is from above. The radiation from a blackbody (BB) radiation source is modulated by a rotary chopper (CH). The gold-coated focusing mirror (FM) images the aperture of the blackbody onto the focal plane of the polarimeter (P). Three rays are shown. We vary the angle of incidence of the radiation at the aluminum mirror (AM) by rotating this mirror and physically moving the polarimeter. Both AM and P are mounted upon rotary milling tables, and the polarimeter mount has two additional translational degrees of freedom. As described in Section 3, we were able to measure the polarization introduced by the reflection at the AM.

the experiment. Our radiation source was a blackbody cavity ( $T \sim 1000$  K) with a 12-mm aperture. A chopper wheel near the blackbody aperture modulated the signal at 20 Hz. We used a gold-coated concave spherical mirror (6" diameter), located 2.7 m from the blackbody aperture, to focus the light onto the polarimeter ( $15^\circ$  angle of incidence). The aluminum mirror, located 0.9 m from the gold mirror, then reflected the radiation toward the polarimeter, which was placed 0.45 m from the aluminum mirror. The angle of incidence at the aluminum mirror could be varied as described in the caption to Fig. 1. We made nine polarization measurements at each of three angles of incidence at the aluminum mirror:  $15^\circ$ ,  $30^\circ$ , and  $45^\circ$ .

After entering the polarimeter, the radiation passed through a birefringent quartz half-wave plate. Rotation of the half-wave plate served to rotate the plane of polarization. A vertical grid in the optical path after the half-wave plate split the beam into its two polarization components, and two  $^3\text{He}$ -cooled bolometers, one for each polarization component, detected the power of the radiation.

A single polarization measurement consisted of measuring the chopped signals at each of 12 half-wave plate angles, with a  $15^\circ$  rotation between successive half-wave plate positions. The measured signals were then normalized and combined into the polarization signal, which is the difference of the two signals divided by their sum.<sup>19</sup> The polarization signal is sinusoidal, with the amplitude giving the magnitude of the linear polarization and the phase giving the polarization angle (i.e., the direction of the  $E$  vector of the radiation). Our convention is that ver-

tical  $E$  vector corresponds to zero polarization angle, with the angle increasing in the counterclockwise direction as viewed by the polarimeter.

The polarimeter was originally built for operation at  $270 \mu\text{m}$  with a sapphire half-wave plate.<sup>19</sup> It was then rebuilt for observations at  $100 \mu\text{m}$  with a quartz half-wave plate.<sup>20</sup> For our study we used a quartz half-wave plate of thickness 4 mm. Our passband was defined by a  $280\text{-}\mu\text{m}$  capacitive mesh low-pass filter<sup>21</sup> and the  $400\text{-}\mu\text{m}$  cutoff of the Winston light concentrators.<sup>22,23</sup> The design of the polarimeter and the technique that we used to obtain the polarization signal are discussed more fully by Dragovan<sup>19</sup> and by Novak *et al.*<sup>20</sup>

We next describe the procedure that we used to analyze these measured polarization signals. For each angle of incidence we performed a least-squares fit to determine a pair of normalized Stokes parameters ( $q$ ,  $u$ ) for that angle of incidence. See Novak *et al.* for a description of how one uses the polarization signal to derive the normalized Stokes parameters.<sup>20</sup>

Optical elements other than the aluminum mirror can induce polarization at submillimeter wavelengths. We therefore assume that the measured normalized Stokes parameters are a sum of two components. The first component represents the systematic polarization, i.e., the polarization induced by the other optical elements. It is a vector with a magnitude and a direction that are independent of the angle of incidence at the aluminum mirror. The second component corresponds to the polarization that arises from the reflection by the aluminum mirror.

To separate these two components we perform a second least-squares fit to determine four parameters: one pair of normalized Stokes parameters to represent the systematic polarization and another pair that is related to the magnitude and the direction of the polarization by reflection. This fit takes the functional form

$$q(\theta) = a_q + b_q \sin \theta \tan \theta, \quad (4a)$$

$$u(\theta) = a_u + b_u \sin \theta \tan \theta, \quad (4b)$$

where  $\theta$  is the angle of incidence at the aluminum mirror,  $q(\theta)$  and  $u(\theta)$  are the measured sets of three values,  $a_q$  and  $a_u$  are the Stokes parameters of the systematic polarization, and the terms that involve  $b_q$  and  $b_u$  are the contributions to the measured Stokes parameters that are due to the reflection from the aluminum mirror. Because we have only three terms in each fit, we assume that the polarization-by-reflection component has the same functional form as what is theoretically expected, i.e., proportional to  $\sin \theta \tan \theta$  (see Section 2).

Figure 2 shows a plot of the data, together with the results of the above fits. The systematic polarization, subtracted from the plotted points, has a magnitude of 0.88% and a polarization angle of  $-32^\circ$ . The dotted curve represents the magnitude of the polarization caused by the reflection from the aluminum mirror, as determined by the fit. We also show

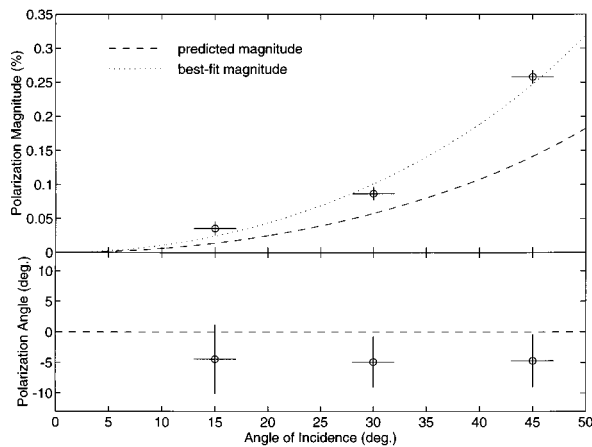


Fig. 2. Plots of magnitude and direction of the polarization induced by the reflection from the aluminum mirror, as a function of angle of incidence. The measurements are represented by circles and are plotted with their associated horizontal and vertical errors. They have been corrected for a systematic offset in the polarization as described in Section 3. Top, the dashed curve represents the theoretically predicted magnitude of the polarization, and a best-fit polarization magnitude is shown as a dotted curve. Bottom, the polarization angle  $0^\circ$  corresponds to the (theoretically expected) vertical direction. A description of the fitting technique used in determining the systematic offset and best-fit curve appears in Section 3.

the theoretical prediction (dashed curve), calculated as described in Section 2. The lower section of the figure shows the polarization angle for each angle of incidence. Vertical polarization corresponds to a polarization angle of  $0^\circ$ , with angle increasing counter-clockwise as seen by the polarimeter. The error in the polarization magnitude is a statistical error calculated from the variance in the raw data. For the polarization angle we estimate that there is a systematic error of  $4^\circ$  introduced by our method of determining the phase of the polarization signal that corresponds to vertical polarization. We combine this systematic error in quadrature with the statistical error in the polarization angle to determine the total error in the polarization angle.

#### 4. Discussion

The two curves shown in the upper plot of Fig. 2 differ by a statistically significant amount. The best-fit curve has a coefficient of 0.35%, whereas theory predicts a coefficient of  $(0.20 \pm 0.02)\%$  (see Section 2). However, for each of the three angles of incidence we measure a direction that is consistent with vertical, in agreement with the prediction. Although the functional form of the polarization magnitude was constrained, the direction of the polarization was not constrained. From the agreement between the measured and the predicted directions we conclude that we did in fact measure the polarization by reflection from the aluminum mirror. We next discuss several possible explanations for the discrepancy between the predicted and the measured polarization magnitudes and conclude that scattering and absorptive

losses owing to surface roughness are the most likely explanations.

We consider first the effect of surface preparation. The machining of the aluminum left a series of concentric circular grooves on the surface. The resultant surface errors, which we estimate to have a rms value (hereafter referred to as  $\Delta$ ) in the range of  $0.5\text{--}2.5\ \mu\text{m}$ , can give rise to Ruze scattering losses<sup>16</sup> of as much as 2%. If one polarization component is preferentially Ruze scattered, the measured polarization by reflection will be significantly different from that theoretically predicted.

In addition to scattering loss owing to surface roughness, the circular groove pattern can give rise to absorptive losses. Recall that  $\delta = 0.1\ \mu\text{m}$ ,  $\lambda = 320\ \mu\text{m}$ , and  $\Delta$  is estimated to be no less than  $0.5\ \mu\text{m}$ . It has been shown that, for  $\lambda \gg \delta$  and  $\Delta \geq 5\delta$ , the normal-incidence absorptivity can increase by as much as 70% of the ordinary skin effect value.<sup>15</sup> Inasmuch as the polarization that is due to oblique reflection is proportional to the normal-incidence absorptivity, our measured polarization could be significantly affected.

We next consider whether we could have detected radiation reflected by the aluminum mirror holder during the  $45^\circ$  angle-of-incidence measurement, which we did not see during the  $15^\circ$  or  $30^\circ$  measurements because of the decreased projected width of the mirror. At a  $45^\circ$  angle of incidence the FWHM of the polarimeter's beam was just under half of the projected horizontal width of the mirror and one third of the mirror's height. Furthermore, we estimate that intensity of the beam at the mirror's edge was no more than 5% of the peak beam intensity.

At first it would appear that this stray radiation could contribute significantly to the measured polarization, as the surface of the mirror holder is parallel to the aluminum mirror surface (the focusing mirror has a similar kind of holder). However, our choices for the sizes and positions of our mirrors prevent any part of our beam that does not reflect off the aluminum mirror from specularly reflecting back to the blackbody source. Thus the only stray, chopped radiation that enters the polarimeter's beam must be diffracted by at least one of the mirror holders. We estimate that approximately 0.01% of the measured flux from the blackbody arrives via such diffracted paths. As this diffracted radiation is most likely not completely polarized, its effect on our measurement is probably negligible.

Finally, we revisit the question of whether a correction that is due to the anomalous skin effect could be important. Dingle<sup>12</sup> (see also Reuter and Sondheimer<sup>11</sup>) tabulates the absorption at normal incidence that arises from the anomalous skin effect for a wide range of conductivities and submillimeter and far-infrared wavelengths. For the conditions ( $\sigma$ ,  $\omega$ ,  $v_F$ , and room temperature) of our experiment, we find that the ordinary and the anomalous skin effect theories predict the same absorption to within a few percent, for normal incidence. Quantum corrections to the anomalous skin effect can arise,<sup>13</sup> but for our

particular case these corrections are negligible.<sup>14</sup> Given the lack of an anomalous skin effect correction at normal incidence, it is reasonable to assume that the anomalous skin effect does not affect the polarization by reflection for moderate angles of incidence. (For wavelengths on the order of tens of micrometers, or for very low temperatures, the anomalous skin effect is important.)

## 5. Conclusions

We conclude that polarization induced by the mirrors of an off-axis telescope will not be a major source of systematic error for submillimeter- and millimeter-wavelength polarimetric observations. At submillimeter wavelengths the effect should be of the order of a few tenths of a percent for an off-axis system that contains multiple oblique reflections with angles of incidence of the order of 15°–45°.<sup>24</sup> For example, we would predict that a telescope with three 45° reflections would have an instrumental polarization of 0.4% at 320  $\mu\text{m}$ . This result roughly applies to all aluminum alloys, as they all have the same bulk conductivity to within  $\sim 25\%$  at room temperature.<sup>25</sup> For millimeter wavelengths the effect will be even smaller. Even as  $\omega$  increases into the far-infrared regime the polarization-by-reflection effect should be manageably small. Our results show that off-axis telescopes should not be overlooked as useful for submillimeter and millimeter polarimetry. Finally, our study should permit better estimates of the far-infrared, submillimeter, and millimeter polarization introduced by oblique reflections in any telescope.

This study was supported by NASA award NAG2-1081, by the Center for Astrophysical Research in Antarctica [National Science Foundation (NSF) Science and Technology Center award OPP 89-20223], and by NSF career award OPP 9618319. We thank R. Hildebrand for lending us the polarimeter, D. Schleuning for donating the low-pass filter, and E. Wollack, M. Dragovan, and J. Peterson for helpful discussions.

## References

1. R. H. Hildebrand, J. L. Dotson, C. D. Dowell, S. R. Platt, D. Schleuning, J. A. Davidson, and G. Novak, "Far-infrared polarimetry," in *Airborne Astronomy Symposium on the Galactic Ecosystem: From Gas to Stars to Dust*, M. R. Haas, J. A. Davidson, and E. F. Erickson, eds., Vol. 73 of ASP Conference Series (Astronomical Society of the Pacific, San Francisco, Calif., 1995), pp. 97–104.
2. L. Spitzer, *Physical Processes in the Interstellar Medium* (Wiley, New York, 1978).
3. R. H. Hildebrand, J. A. Davidson, J. Dotson, D. F. Figer, G. Novak, S. R. Platt, and L. Tao, "Polarization of the thermal emission from the dust ring at the center of the galaxy," *Astrophys. J.* **417**, 565–571 (1993).
4. D. P. Gonatas, X. D. Wu, G. Novak, and R. H. Hildebrand, "Systematic effects in the measurement of far-infrared linear polarization," *Appl. Opt.* **28**, 1000–1006 (1989).
5. D. A. Schleuning, C. D. Dowell, R. H. Hildebrand, S. R. Platt, and G. Novak, "Hertz, a submillimeter polarimeter," *Publ. Astron. Soc. Pac.* **109**, 307–318 (1997).
6. E. J. Konopinski, *Electromagnetic Fields and Relativistic Particles* (McGraw-Hill, New York, 1981).
7. E. J. Wollack, "A measurement of the degree scale cosmic background radiation anisotropy at 27.5, 30.5, and 33.5 GHz," Ph.D. dissertation (Princeton University, Princeton, N.J., 1994), pp. 147–156.
8. J. Xu, A. E. Lange, and J. J. Bock, "Far-infrared emissivity measurements of reflective surfaces," in *Submillimetre and Far-Infrared Space Instrumentation*, Proceedings of the 30th ESLAB Symposium (ESTEC, Noordwijk, The Netherlands, 1996), pp. 69–72.
9. H. London, "The high-frequency resistance of superconducting tin," *Proc. R. Soc. London Ser. A* **176**, 522–533 (1940).
10. A. B. Pippard, "The surface impedance of superconductors and normal metals. II. The anomalous skin effect in normal metals," *Proc. R. Soc. London Ser. A* **191**, 385–399 (1947).
11. G. E. H. Reuter and E. H. Sondheimer, "The theory of the anomalous skin effect in metals," *Proc. R. Soc. London Ser. A* **195**, 336–364 (1948).
12. R. B. Dingle, "The anomalous skin effect and the reflectivity of Metals. I," *Physica* **19**, 311–347 (1953).
13. A. P. van Gelder, "Quantum corrections in the theory of the anomalous skin effect," *Phys. Rev.* **187**, 833–842 (1969).
14. S. Iganaki, E. Ezura, J.-F. Liu, and H. Nakanishi, "Thermal expansion and microwave surface reactance of copper for the normal to anomalous skin effect region," *J. Appl. Phys.* **82**, 5401–5410 (1997).
15. S. P. Morgan, Jr., "Effect of surface roughness on eddy current losses at microwave frequencies," *J. Appl. Phys.* **20**, 352–362 (1949).
16. J. Ruze, "The effect of aperture errors on the antenna radiation pattern," *Nuovo Cimento Suppl.* **9**, 364–380 (1953).
17. "Aluminum 6061," in *Alloy Digest*, filing code Al-205 (Engineering Alloy Digest, Upper Montclair, N.J., 1973), Part 1.
18. H. P. Myers, *Introductory Solid State Physics* (Taylor & Francis, Bristol, Pa., 1981).
19. M. Dragovan, "Submillimeter polarization in the Orion nebula," *Astrophys. J.* **308**, 270–280 (1986).
20. G. Novak, D. P. Gonatas, S. R. Platt, and R. H. Hildebrand, "A 100- $\mu\text{m}$  polarimeter for the Kuiper airborne observatory," *Proc. Astron. Soc. Pac.* **101**, 215–224 (1989).
21. S. E. Whitcomb and J. Keene, "Low-pass interference filters for submillimeter astronomy," *Appl. Opt.* **19**, 197–198 (1980).
22. R. Winston, "Light collection within the framework of geometrical optics," *J. Opt. Soc. Am.* **60**, 245–247 (1970).
23. R. Winston and W. T. Welford, "Geometrical vector flux and some new nonimaging concentrators," *J. Opt. Soc. Am.* **69**, 532–536 (1979).
24. T. Renbarger, J. L. Dotson, and G. Novak, "An estimate of telescope polarization for the SPARO experiment," in *Astrophysics from Antarctica*, G. Novak and R. H. Landsberg, eds., Vol. 141 of ASP Conference Series (Astronomical Society of the Pacific, San Francisco, Calif., 1998), pp. 205–207.
25. "Aluminum 2024," and "Aluminum 7075," in *Alloy Digest*, filing codes Al-23 and Al-179 (Engineering Alloy Digest, Upper Montclair, N.J., 1973), part 1.